JACS
JOURNAL OF THE AMERICAN CHEMICAL SOCIETY
Article
pubs.acs.org/JACS

Does Cation Size Affect Occupancy and Electrostatic Screening of the Nucleic Acid Ion Atmosphere?

Magdalena Gebala,[†] Steve Bonilla,[‡] Namita Bisaria,[†,⊥] and Daniel Herschlag*[,†,§,∥]

[†]Department of Biochemistry, Stanford University, Stanford, California 94305, United States
[‡]Department of Chemical Engineering, Stanford University, Stanford, California 94305, United States
[§]Department of Chemistry, Stanford University, Stanford, California 94305, United States
[∥]ChEM-H Institute, Stanford University, Stanford, California 94305, United States

Supporting Information

ABSTRACT: Electrostatics are central to all aspects of nucleic acid behavior, including their folding, condensation, and binding to other molecules, and the energetics of these processes are profoundly influenced by the ion atmosphere that surrounds nucleic acids. Given the highly complex and dynamic nature of the ion atmosphere, understanding its properties and effects will require synergy between computational modeling and experiment. Prior computational models and experiments suggest that cation occupancy in the ion atmosphere depends on the size of the cation. However, the computational models have not been independently tested, and the experimentally observed effects were small. Here, we evaluate a computational model of ion size effects by experimentally testing a *blind* prediction made from that model, and we present additional experimental results that extend our understanding of the ion atmosphere. Giambasu et al. developed and implemented a three-dimensional reference interaction site (3D-RISM) model for monovalent cations surrounding DNA and RNA helices, and this model predicts that Na^+ would outcompete Cs^+ by 1.8−2.1-fold; i.e., with Cs^+ in 2-fold excess of Na^+ the ion atmosphere would contain an equal number of each cation (*Nucleic Acids Res.* **2015**, *43*, 8405). However, our ion counting experiments indicate that there is no significant preference for Na^+ over Cs^+. There is an ∼25% preferential occupancy of Li^+ over larger cations in the ion atmosphere but, counter to general expectations from existing models, no size dependence for the other alkali metal ions. Further, we followed the folding of the P4−P6 RNA and showed that differences in folding with different alkali metal ions observed at high concentration arise from cation−anion interactions and not cation size effects. Overall, our results provide a critical test of a computational prediction, fundamental information about ion atmosphere properties, and parameters that will aid in the development of next-generation nucleic acid computational models.

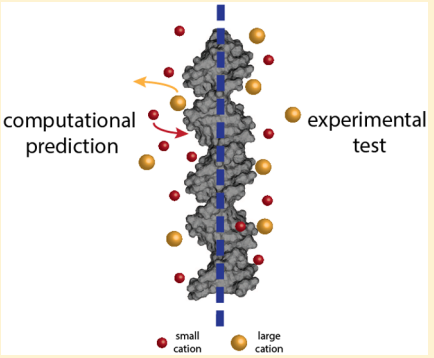

INTRODUCTION

The polyelectrolyte nature of nucleic acids renders their structure, interactions, and function strongly dependent on the presence of ions. DNA condensation,[1−4] packing of genomes into viral capsids,[2,5,6] and the folding of functional RNAs[7−10] require the repulsive forces between closely packed phosphate residues to be abated by positively charged cations. The vast majority of the cations that play this role are not site-specifically bound but rather are part of a mobile cloud of ions surrounding molecules, referred to as the ion atmosphere. Thus, the ion atmosphere is a critical structural, dynamic, and energetic component of nucleic acids, and dissection of its properties and behavior is necessary for understanding nucleic acid structure, dynamics, and function.

Yet, progress in experimental study of the ion atmosphere has been difficult,[11] in part because there is no unique structure for this highly mobile cloud. An additional complication is that the ions in this atmosphere are under the influence of long-range electrostatic forces and do not conform to the mass action laws that are the basis for our understanding of nearly all ligand-binding interactions.[12−14] Consequently, distinct theoretical frameworks have been needed and have been heavily relied upon. These frameworks date back to Manning's early counterion condensation model[15,16] and include Poisson−Boltzmann (PB) theory[17−19] and more recent coarse-grain and atomistic approaches that are currently in use.[20−26]

Indeed, progress in computational simulations has made it possible to obtain atomic-level descriptions of the ions in the ion atmosphere, including their positions with respect to the nucleic acid and one another and their hydration status.[27−33] These simulations typically reveal cations in helical grooves, with a size dependence to this occupancy,[29,31,32,34−39] and greater accumulation of smaller cations around phosphoryl oxygen atoms.[30,31,37,40,41] Thus, computational approaches have provided general support for cation size as an important

Received: May 3, 2016
Published: August 1, 2016

DOI: 10.1021/jacs.6b04289
J. Am. Chem. Soc. 2016, 138, 10925−10934

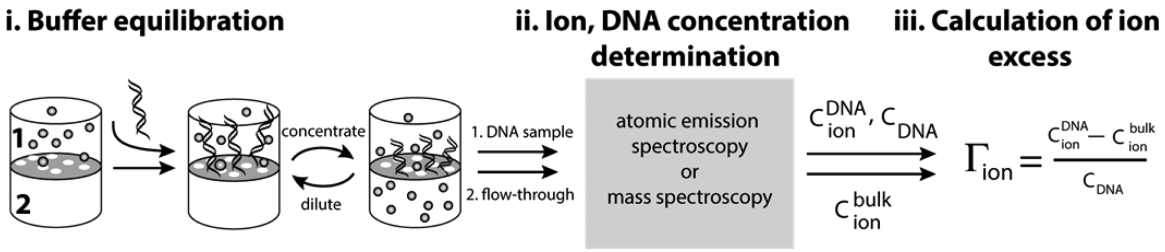

Figure 1. Scheme of the buffer equilibration–mass spectroscopy experiment, referred to as "ion counting" herein. The scheme is adapted from refs 48, 51. A detailed description of the ion counting methodology is presented in Experimental Methods and refs 48, 51, 58.

determinant of cation position in and occupancy of the ion atmosphere and of the ion atmosphere's ability to screen nucleic acid charge.[31,36,37,41,42]

Nevertheless, whether this information is accurate, or not, can only be gauged empirically, through specific predictions that are made by these models and subsequently tested experimentally.[39,41,43,44] Recently, York and colleagues[41] quantitatively computed the ion atmosphere occupancy for a series of monovalent cations using a three-dimensional reference interaction site model (3D-RISM) based on the *ff10* AMBER force field for nucleic acids,[45] Joung and Cheatham ion potentials,[46] and the SPC/E solvation model.[47] Importantly, in addition to providing comparisons to previously measured cation occupancies,[48] this work also provided a blind prediction for the ability of Cs^+ to compete with smaller alkali metal cations for occupancy in the ion atmosphere. In other words, as Cs^+ occupancy had not been previously determined experimentally, its measurement would represent a true test of the computational model. As for the test of any model, disagreement would require the model to be rejected or modified, whereas agreement would allow the model to stand, with the expectation that the model would be subject to additional tests in the future.

An experimental approach that has been particularly effective for testing theoretical predictions concerning the ion atmosphere is ion counting.[48−51] The most basic expectation from polyelectrolyte theories is that the ion atmosphere, as a whole, neutralizes nucleic acids such that the overall charge of a nucleic acid and the ions that constitute the ion atmosphere sum to zero. This prediction has been verified by ion counting experiments that used buffer-exchange atomic emission spectroscopy (BE-AES; Figure 1) to fully account for the ion atmosphere constituents. These experiments also determined the cation accumulation in and anion exclusion from the ion atmosphere, quantities that also can be obtained from polyelectrolyte theories[48,49,51,52] (see also ref 50).

Prior ion counting studies[48] suggested, consistent with theoretical expectations, that smaller cations preferentially occupy the ion atmosphere around DNA helices. Studies on the relaxation of short DNA helices attached by a short, flexible linker[53] and other experiments[54−57] revealed an analogous trend. However, there are limitations to each of these measurements. The observed differences in ion association of the alkali metal ions around the double-stranded DNA were very small, less than 20%, and in general difficult to distinguish from experimental uncertainty.[48,54] The relaxation studies,[53] we now recognize based on very recent studies,[51] could have been affected by nonideal behavior of simple electrolytes (i.e., ion–ion correlations and ion clustering) at the high salt concentrations required for these experiments, Thus, the conclusions from these and other experimental studies[54−57] require further investigation.

The blind predictions by York and colleagues have allowed us to carry out an experimental test of a quantitative *prediction* from theory.[41] We show, counter to the theoretical prediction, that Cs^+ is not excluded from the ion atmosphere of DNA and RNA helices relative to Na^+, thereby providing information required for progress toward accurate electrostatic models of nucleic acids and their electrostatics. Given the importance of basic knowledge about the ion atmosphere, and the limited and generally complex experimental information available, we also took advantage of recent enhancements in the capabilities of ion counting to expand prior studies of cation competition for ion atmosphere occupancy.[48] Our results confirm the preferential ion atmosphere occupancy of Li^+, consistent with the current 3D-RISM model[41] and prior experimental studies,[48] but show that there is no significant size preference for other alkali metal ions. Finally, we provide evidence, following folding of P4–P6 RNA, that different effects on folding at high salt concentrations arise from nonideal behavior of simple electrolytes that causes differential electrostatic screening, rather than from cation size effects.

EXPERIMENTAL METHODS

Reagents. DNA and RNA oligonucleotides were purchased from IDT (Integrated DNA Technologies, USA). The following DNA sequences were used S1: $_{5'}$GGT GAC GAG TGA GCT ACT GGG CGG$_{3'}$ and S2: $_{5'}$CCG CCC AGT AGC TCA CTC GTC ACC$_{3'}$. RNA sequences were the same except for containing uracil instead of thymine bases. All salts were of the highest purity (TraceSELECT or BioXtra, Sigma-Aldrich USA). All solutions were prepared in high purity water, ultralow TOC biological grade (Aqua Solutions, USA).

Preparation of DNA and RNA Samples. DNA and RNA constructs used in this study were duplexes assembled from chemically synthesized oligonucleotides. The DNA construct was the same as used in previous ion counting studies.[48] Oligonucleotides were purified by reverse-phase HPLC (XBridge Oligonucleotide BEH C18; Waters, MA) and desalted using centrifugal Amicon Ultra-3K filers (Millipore, MA). Equimolar complementary strands (0.1–0.3 mM) were annealed in 20 mM Na-EPPS (sodium 4-(2-hydroxyehyl)piperazine-1-propane-sulfonic acid), pH 8.4; samples were incubated at 70 °C for 1 min and gradually cooled to ambient temperature over 1 h. Nondenaturing polyacrylamide gel electrophoresis (PAGE, stained by Stains-All, Sigma-Aldrich, USA) showed no detectable single stranded DNA and RNA in samples, corresponding to >90% duplex.

Buffer Equilibration-Inductively Coupled Plasma Mass Spectroscopy (BE-ICP MS). Buffer equilibration for DNA and RNA was carried out using Amicon Ultracel-30K filters (Millipore, MA), replacing Microcon YM-30 (Millipore, MA) used previously.[48] Salt samples were prepared in 2 mM Na-EPPS, Li-EPPS or Mg-EPPS, pH 8.5 and their concentrations were determined by ICP MS. The initial 500 μL of 0.2 to 2 mM 24-bp DNA or 24-bp RNA samples, with the salt of interest, was spun down to ~100 μL at 7000*g* in Amicon Ultracel-30K filters (Figure 1, i) at 4 °C (to minimize solution

DOI: 10.1021/jacs.6b04289
J. Am. Chem. Soc. 2016, 138, 10925−10934

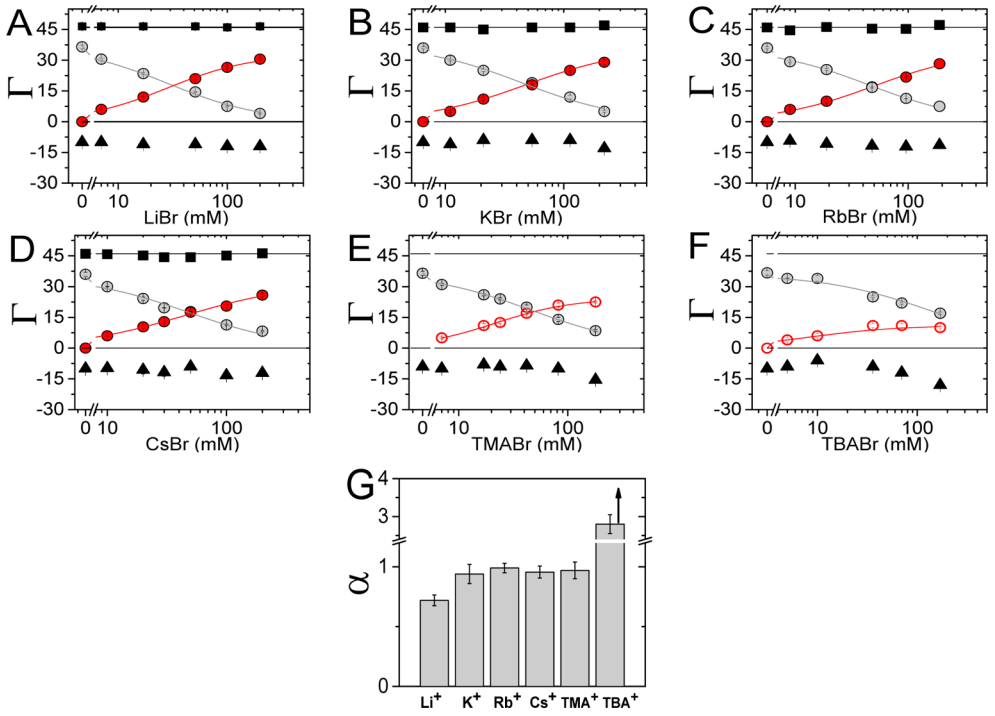

Figure 2. Competitive association of monovalent cations with a 24-bp DNA duplex. (A–F) The number of ions in the ion atmosphere for a series of cations (red circles, Li^+, K^+, Rb^+, Cs^+, TMA^+ and TBA^+) versus Na^+ (gray circles; $[Na^+]$ = 50 mM, except A and F where $[Na^+]$ = 40 mM); excluded Br^- anion is represented by the black triangles. The total charge of the ion atmosphere summed from the individual ion measurements is shown as the black squares, and the lines at Γ = +46 represent the charge needed to neutralize the total DNA charge of −46. Cations that could not be directed assayed (TMA^+ and TBA^+) were estimated from the number of Na^+ and Br^- ions and assuming overall charge neutrality and are shown as open symbols. Solid lines (red and gray) are fits with the Hill equation and provide an empirical guide. Errors are the standard deviation of all measurements. (G) Cation competition constants for monovalent cations against Na^+. $\alpha = \frac{\beta}{[BG]}$ (eq 5), where $\beta = [M]_{1/2}$ is the competition constant of the competing cation defined by eq 4 and [BG] is the concentration of the background cation, Na^+. The arrow for the α value for TBA^+ depicts that this value is a limit. Each data point in panels A–F is the average of 3–5 independent measurements. See Tables S1–S7 in Supporting Information for raw data.

evaporation).[58] As shown previously,[51] equilibration between ions associated with nucleic acids and the bulk ions was completed after five rounds of the buffer exchange without any loss of the DNA or RNA; no DNA or RNA was detected in flow-through samples, as determined by ICP MS, assaying the phosphorus content.

Ion Counting. Inductively coupled plasma mass spectrometry (ICP-MS) measurements were carried out using a XSERIES 2 ICP-MS (Thermo Scientific, USA), which has a higher precision and a lower detection limit compared to IRIS Advantage 1000 radial ICAP Spectrometer (Thermo Jarrell Ash) used in earlier studies.[48] Additionally, the ICP MS can assay halogens, allowing us to measure anion exclusion from the ion atmosphere and in turn to independently calculate the total charge of the atmosphere, a value that provides a powerful quality control by comparison the theoretical expectation of overall charge neutrality. Herein, ion counting measurements were carried out with bromide salts, as the detection of Br^- anion by ICP MS has highest accuracy and precision compared to other halogens.

Samples were analyzed as described in ref 51. Briefly, aliquots (5–20 μL) of DNA- or RNA-containing sample, the flow-through from the final equilibration, and the equilibration buffer were diluted to 5 mL in 15 mL Falcon tubes with water. Dilution factors, the ratio of diluted to total sample volume, were used to maintain sample concentrations within the linear dynamic range of detection.[51] Calibrations were carried out using standards from SpexCertiPrep (USA). Quality control samples, containing each element of interest at 50 μM, were assayed every ten samples to estimate measurement precision.[59] To minimize memory effects in Br^- detection, a solution of 5% ammonium hydroxide in highly pure, ion-free water (Mili Q) was used as a wash-out solution between measurements.[60]

Tetramethylammonium (TMA^+) and tetrabutylammonium (TBA^+) were not directly assayed by ICP-MS. (Carbon and nitrogen atoms, which are present in TMA^+ and TBA^+, could in principle be used to determine the concentration, but their presence in DNA and RNA precludes direct determination of the cations.) In these cases, the number of accumulated cations was calculated based on the charge neutrality principle from the measured number of depleted Br^- ions and the total charge of 24-bp DNA (eq 1), as established by prior results.[48,51]

$$\sum q_i \Gamma_i = -q_{NA} \quad (1)$$

In eq 1, q_i indicates the charge of ionic species i, Γ_i is the preferential interaction coefficient (i.e., the number of associated ion), and q_{NA} is the charge of the DNA or RNA, which is equal to −46 for the 24-bp DNA and 24-bp RNA studied herein. Calculated cation counts are represented by open instead of closed circles in figures throughout the text.

For each ion counting data point reported, at least three measurements were made on three different days with independently prepared samples. Errors are the standard deviation of all measurements.

The number of associated ions around the 24-bp DNA and 24-bp RNA is reported here as a preferential interaction coefficient[61] Γ_i (i = + or −, indicating cation or anion, respectively), where Γ_i is the difference in the ion concentration between the equilibrated nucleic acid-containing sample (c_{ion}^{NA}) and the bulk solution (c_{ion}^{bulk}), divided by the DNA or RNA concentration (c_{NA}; determined by phosphorus measurements using ICP MS) (eq 2).

DOI: 10.1021/jacs.6b04289
J. Am. Chem. Soc. 2016, 138, 10925–10934

$$\Gamma_i = \frac{C_{ion}^{NA} - C_{ion}^{bulk}}{C_{NA}} \quad (2)$$

For DNA or RNA, the cation preferential interaction coefficient, Γ_+, is expected to be greater than zero, indicating their accumulation around the negatively charged polyelectrolytes, and Γ_- for an anion is expected to be less than zero due to repulsive interactions with the DNA or RNA.

Quantification of Cation Competition. To evaluate differences in the association between two cation species with the 24-bp DNA and 24-bp RNA, we used the same method as described previously.[48] Briefly, the number of competing cations (CC) and background cations (BC) around the DNA was measured over a range of CC concentrations at a given constant concentration of BC (see Figures 2, 4, 5, and 8 below). The competition constant (β) was defined as the concentration of competing cation at which half of the number of BC associated with the DNA or RNA in the absence of the CC are replaced by the CC. The competition constant (β) was computed via an empirical two-state model as the midpoint ($[M]_{1/2}$) of the background cation association, using Hill analysis:

$$\Gamma = \Gamma_1 + \frac{(\Gamma_0 + \Gamma_1)}{1 + ([M]/[M]_{1/2})^n} \quad (3)$$

$$[M]_{1/2} = \beta \quad (4)$$

where Γ is the number of associated background cations at a given concentration of the competing cation, $[M]$, Γ_0 and Γ_1 are the number of associated background cations in the absence of the competing cation and extrapolated to infinite competing cation, respectively, and n is the Hill coefficient. Hill analysis is complex for polyelectrolytes[62] and we use it here as an empirical description of the competition behavior.

P4−P6 RNA Preparation and Single Molecule FRET (smFRET) Experiments. A P4−P6 RNA construct for smFRET studies was prepared as previously reported.[51,63] The biotinylated sample was diluted to a concentration of ∼50 pM and flowed onto a BSA-streptavidin-coated quartz slide for surface attachment and imaging. smFRET experiments were carried out in 40 mM Na-MOPS, pH 7.0, 0.1 mM Na-EDTA with the salt of interest and with an oxygen scavenging system of 2.0 mM Trolox, 60 units/mL protocatechuate-3,4-dioxygenase (PCD) and 100 mM protocatechuic acid (PCA). Images were taken using a custom total internal reflection (TIRF) setup with image acquisition by Andor iXon Ultra camera and the Nikon Elements software at three different acquisition rates: 48, 92, and 145 frames per second (fps). Results were independent of the frame frequency (Figure S1). The FRET traces of individual molecules displayed transitions between two FRET states: a high FRET state of 0.95, corresponding to the folded states, and a low FRET state of ∼0.2 corresponding to the unfolded state.[64] (smFRET data assessment is shown in Figures S2-1 to S15-3.) To determine equilibrium and folding rate constants, FRET traces were analyzed with the SMART analysis package, as described previsouly.[63,65]

RESULTS

Assessing Preferential Ion Atmosphere Occupancy of Cations via Competitive Association. We first studied the competitive association of monovalent cations with a 24-bp model DNA in the presence of Br^- as the counterion (Figure 2). A series of competing monovalent cations were titrated at various concentrations (5−200 mM) into a 50 mM or 40 mM solution of Na^+ as a background cation (BG, see Experimental Methods). In the absence of a competing cation, there are 37 ± 1 Na^+ ions associated with the DNA and 10 ± 1 Br^- ions excluded, in agreement with prior measurements.[51] Increasing concentration of the competing cation led to an increase in the number of that cation around the DNA and a decrease in the number of background Na^+ cations, with little or no change in the number of excluded anions.

The ion atmosphere screens the charge of nucleic acids, and the total number of ions within the ion atmosphere (i.e., the number of accumulated cationic species and the number of excluded anions) should be equal in number and opposite in sign to the charge of the macromolecule: here a 24-bp DNA or 24-bp RNA of charge −46. In all cases where both the cation and anion could be directly measured, the calculated total charge agreed well with the charge of the DNA and RNA (Figures 2A−D, Figure 4, and Figure 5 below, +46; squares vs solid black line; see also refs 48, 51). If a cation or an anion could not be directly assayed, we assumed overall charge neutrality, based on the above-noted results, and used this relationship (eq 1) to calculate the accumulation or depletion of that cation or anion; these values are represented as open symbols (circles for cations and triangles for anions; e.g., Figures 2E, 2F, and Figure 8B).

To estimate how much stronger a given cation species interacts with the DNA or the RNA, relative to a given background cation, we introduce the unitless parameter α, defined as

$$\alpha = \frac{\beta}{[BG]} \quad (5)$$

where β is the cation competition constant, i.e., the concentration of competing cation at which half of the initial number of background cations is replaced by the competing cation (eq 4, Experimental Methods), and [BG] is the concentration of the background cation. The relative preferential cation occupancy from the data of Figure 2A−F is summarized in Figure 2G in terms of α. There is small but significant preference for Li^+ over Na^+ (α = 0.72 ± 0.05). However, K^+, Rb^+, Cs^+, and TMA^+ all gave α values of unity, within error, indicating no net preferential ion atmosphere occupancy between these ions (α = 0.95−0.99; Table S7). We expected, nevertheless, that a sufficiently large cation with a low charge density would have a limited ability to closely approach the duplex and thus have a lower ability to compete with other cations for occupancy of the ion atmosphere. To investigate a cation larger than Cs^+ (3.06 Å, hydrated ion radius)[66] and TMA^+ (3.7 Å),[67,68] we turned to tetrabutylammonium (TBA^+, 4.57 Å).[68] Indeed, we observed approximately 3-fold weaker association of TBA^+ compared to Na^+ (Figure 2F; $\alpha \approx 2.8$).[69]

To further test the observed preference for Li^+, we carried out the converse experiment, titrating varying amounts of Na^+ into a background of 16 or 50 mM Li^+ (Figure S16). The α values were larger than 1, consistent with the preferential association of Li^+ over Na^+ (α = 1.25 ± 0.08 and 1.20 ± 0.07, at 16 and 50 mM Li^+ respectively). We also counted Li^+ ions around the 24-bp DNA in the absence of a secondary cation over the concentration range 10−250 mM. There was, on average, three more Li^+ cations associated with the DNA compared to Na^+, Rb^+, or Cs^+, and correspondingly fewer excluded anions, consistent with stronger association of Li^+ with the duplex (Figure 3).

As an additional independent test of cation size effects, we carried out cation competition experiments for Li^+, Na^+, and Cs^+ in the presence of a Mg^{2+} background. Again, there were no significant difference between Na^+ and Cs^+ in replacing the divalent cation, but, as above, Li^+ was more efficient at displacing Mg^{2+} (Figure 4; α = 8.6 ± 0.5, 8.7 ± 0.8 and 7.0 ± 0.6 for Na^+, Cs^+, and Li^+, respectively).

DOI: 10.1021/jacs.6b04289
J. Am. Chem. Soc. 2016, 138, 10925−10934

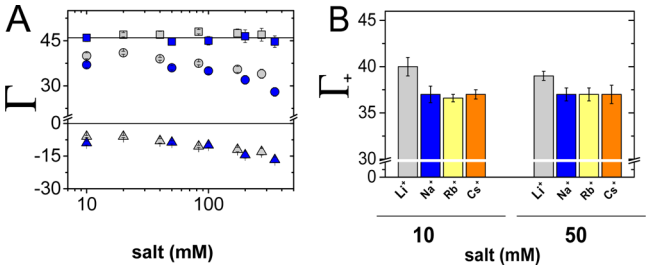

Figure 3. Preferential association of cations with a 24-bp DNA for solutions of individual salts over a range of bulk ion concentrations (10–350 mM). (A) Association of LiBr (gray) and NaBr (blue). Accumulated cations: Li^+ (gray circles) or Na^+ (blue circles); depleted anions: Br^- (triangles). The line at Γ = +46 represents the charge needed to neutralize the total DNA charge of −46. Each data point is the average of three independent measurements. See Table S8 for raw data. (B) The number of accumulated monovalent cations around 24-bp DNA at 10 mM and 50 mM: Γ_{Li^+} was measured herein, and Γ_{Na^+}, Γ_{Rb^+}, Γ_{Cs^+} were taken from ref 51, where the same methodology was used. Error bars as in Figure 2.

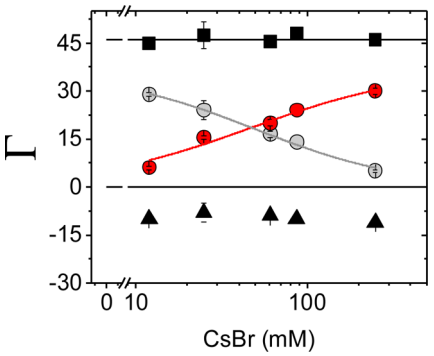

Figure 5. Competitive association of monovalent cations with a 24-bp RNA duplex. The number of ions in the ion atmosphere for Cs^+ (red circles) versus Na^+ (gray circles; [Na^+] = 50 mM); excluded Br^- anion is represented by the black triangles, and the total charge of the ion atmosphere summed from the individual ion measurements is shown as the black squares. The line at Γ = +46 represents the charge needed to neutralize the total RNA charge of −46. The solid line (red and gray) are fits to the Hill equation to provide an empirical guide. Each data point is the average of 3–5 independent measurements. Error bars as in Figure 2. See Table S18 in Supporting Information for raw data.

Competition constants were also predicted by York and colleagues for monovalent cations around an RNA duplex.[41] We therefore carried out ion counting experiments with the RNA duplex for which those predictions were made, and we used Cs^+, as the largest difference was predicted for this cation. We added varying amounts of Cs^+ in a background of 50 mM Na^+ and observed, as we did for DNA (Figures 2D and 2G), no significant differential association of Na^+ versus Cs^+ ($\alpha = 0.99 \pm 0.08$; Figure 5 and Table S18 in SI).

We compare the theoretical predictions and experimental data for both DNA and RNA in the next section and in the Discussion.

Comparison of Experimental Results to Theoretical Results and Bona Fide Blind Predictions. As emphasized in the Introduction, the computation results from York and colleagues[41] provide a rare blind prediction of an ion atmosphere property that can be experimentally tested. The authors benchmarked their 3D-RISM computational model against previous ion counting results with a DNA helix[48] and were able to obtain good agreement (Figure S17). They then used this model, which utilized Joung and Cheatham ion potentials[46] and the SPC/E solvation model,[47] to predict the Cs^+ occupancy around DNA and RNA helices in the presence of Na^+. Specifically, the 3D-RISM model predicted that Na^+ would outcompete Cs^+ by 1.8-fold for the DNA helix investigated and 2.1-fold for the RNA helix; i.e., with Cs^+ in ~2-fold excess of Na^+ the ion atmosphere would contain equal number of each cation.

We carried out ion counting experiments with the DNA and RNA duplex for which those predictions were made. Whereas the computational results were obtained with Cl^- as the counterion, the experiments were carried out with Br^- in order to maximize experimental precision (see Experimental Methods). Nevertheless, previous experiments comparing anion effects[51] and additional controls indicate that there is no difference in cation behavior with Cl^- or Br^- under the conditions of these experiments (Figure S18). We observed no significant differential association of Na^+ versus Cs^+ for either DNA or RNA helices (Figures 2D and 5). Figure 6, comparing the predicted and observed preferential ion atmosphere occupancies (i.e., the α values, eq 5) for all of the cations tested, illustrates the clear difference between the computed correlation with cation size and the observed absence of a difference for all ions other than Li^+.

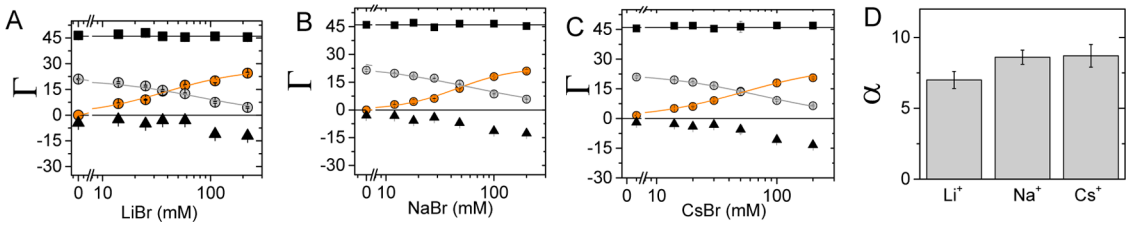

Figure 4. Competitive association of monovalent cations versus Mg^{2+} for a 24-bp DNA duplex. (A–C) The number of ions in the ion atmosphere for a series of monovalent salts: Li^+, Na^+, Cs^+ (orange circles) versus Mg^{2+} (A: [Mg^{2+}] = 5 mM; B and C: [Mg^{2+}] = 6 mM, gray circles); excluded Br^- anions are represented by the black triangles, and the total charge of the ion atmosphere summed from the individual ion measurements is shown as the black squares. The lines at Γ = +46 represent the charge needed to neutralize the total DNA charge of −46. Solid lines (orange and gray) are fits to the Hill equation to provide an empirical guide. (D) Cation competition constants for monovalent cations against Mg^{2+}. $\alpha = \frac{\beta}{[BG]}$ (eq 5), where β is the competition constant of the competing cation, defined in eq 4, and [BG] is the concentration of the background cation, Mg^{2+}. Each data point is the average of three independent measurements. Error bars as in Figure 2. See Tables S15–S17 in Supporting Information for raw data.

DOI: 10.1021/jacs.6b04289
J. Am. Chem. Soc. 2016, 138, 10925–10934

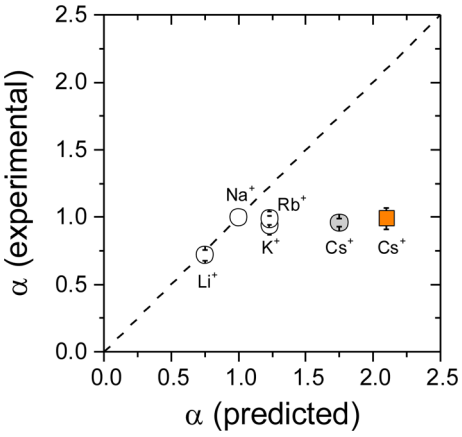

Figure 6. Comparison of experimentally determined versus 3D-RISM computationally determined ion atmosphere cation competition (α values; eq 5). Cations that were computationally estimated, subsequent to prior experimental measurements,[48,51] are shown with open symbols, and those with blind computational predictions[41] by closed symbols. The open and gray symbols are for a 24-bp DNA, and the orange symbol for a 24-bp RNA. Each cation (identified in figure) was competed versus Na^+, so that α is 1 for Na^+ and there is no error. Experimental values shown are for the data obtained herein (Figures 2, 5 and Table S1–S4 and S18), and the prior experimental data are compared to the computational results in Figure S17.

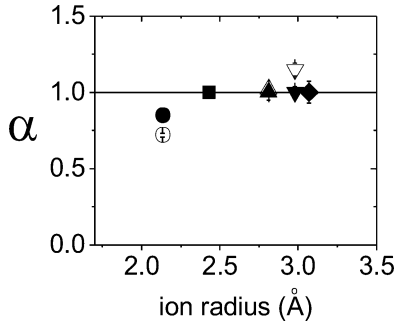

Figure 7. Preferential competition of alkali metal ions as a function of hydrated ion size. Competition constants, α, from data in Figure 2 (closed symbols) and from ref 48 (open symbols) obtained from eq 5. Monovalent cations: Li^+ (circles), Na^+ (squares), K^+ (triangles), Rb^+ (inverted triangles), and Cs^+ (diamond). The radii of the hydrated ions (metal–oxygen bond distances) are from ref 66. The solid line at $\alpha = 1$ is shown as an empirical guide.

In the 3D-RISM model, smaller cations, with higher charge density (e.g., Li^+ and Na^+) have higher occupancy near the phosphoryl groups and are able to penetrate deeper into the minor and major grooves. While this may be the case for Li^+, based on its preferential ion atmosphere occupancy, the *predicted* lower occupancy of Cs^+ is not observed (Figure 6), indicating that there is no experimental support for the physical properties that underlie the 3D-RISM model, specifically the phosphoryl group–cation interactions.[32] These properties appear to be common to other theoretical models,[37−39] although we are not aware of blind predictions that have been made from the other models that would allow their quantitative experimental assessment. As highlighted in the Discussion, new models and new types of experimental tests will be needed to develop and test accurate and predictive models of the ion atmosphere and nucleic acid electrostatics.

Experimental Considerations: Comparison with Prior Ion Atmosphere Occupancy Results. The preferential Li^+ occupancy of the ion atmosphere compared to Na^+ and the absence of a significant preference for Na^+ versus K^+ are consistent with prior ion counting results.[48] However, our results did not match small preferences for Na^+ over Rb^+ and TMA^+ (Figure 7). The prior studies suggested that Rb^+ is disfavored with respect to Na^+ by ~10%, corresponding to α value of 1.10 ± 0.05 and not clearly distinguishable from a value of one given the experimental error of that study. In contrast, the TMA^+ value was α = 1.55 ± 0.04, beyond the error expected for ion counting.[48,51]

The very small discrepancy in the Rb^+ results is likely experimental error from the prior measurement, given that we see consistent values of α = 1.04, 0.94, and 0.98 in three independent experiments. In addition, the current methodology has higher precision and reproducibility (see Experimental Methods and ref 51). These factors, however, cannot account for the larger prior apparent preference for Na^+ over TMA^+. We suspected that this might have arisen from incorrect estimates of the stock solution concentration, as TMA^+ salts are hygroscopic. The following observations support this model. The TMACl used previously was purchased as anhydrous material and the anhydrous molecular weight was presumably used. Correction of the prior ion counting results for hydration of the salt (i.e., correcting to a molecular weight of 181.6 g/mol instead of 109.6 g/mol) results in good agreement with the new data for TMABr, for which the TMA^+ concentration was directly confirmed by ion counting of the stock solution[70] (Figure S19).

Evidence for an Alternative Model for Cation-Size Effects at High Salt Concentrations. Studies of the relaxation of short DNA helices attached by a short, flexible linker[53] and related studies of nucleic acid association and condensation showed stronger effects for smaller cations.[54,56,57,63,71] These studies have been interpreted to support a preferential occupancy of smaller cations in the ion atmosphere and preferential electrostatic screening by those smaller cations. However, a recent experimental study demonstrated additional cation *and* anion accumulation in the ion atmosphere at high salt concentrations for salts with cation–anion pairs that are similar in size.[51] These results together with computational studies[30,72] suggest that ion pairs or clusters within the ion atmosphere and in the bulk of electrolyte solution may alter electrostatic screening of nucleic acids potential. Thus, the model in which the observed cation size dependences at high salt are indirect activity effects, rather than direct effects, arising from preferential anion interactions with cations of different size that then diminish the cation screening ability needed to be tested.

To test whether this activity model could account for the prior cation-size effects observed at high salt concentrations we used series of monovalent salts of varying cation size, Na^+, K^+, Rb^+ and Cs^+, and we varied the anion identity to modulate the salt activity. We first demonstrate that these nonideal effects can alter cation competition for ion atmosphere occupancy at high salt. Subsequently, we show analogous anion-dependent effects on the thermodynamics and kinetics of RNA folding. These findings indicate that the prior cation-size effects cannot be considered as evidence for size-dependent cation occupancy and screening within the nucleic acid ion atmosphere.

In an ion competition experiment with equal bulk concentration of 300 mM CsBr and 300 mM NaBr (Figure 8), there was 2-fold more Na^+ ions accumulated around the 24-

DOI: 10.1021/jacs.6b04289
J. Am. Chem. Soc. 2016, 138, 10925−10934

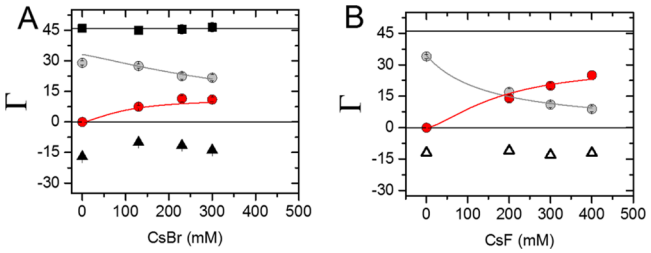

Figure 8. Competitive association of Cs^+ versus Na^+ (300 mM) for a 24-bp DNA duplex. (A) Competitive association of CsBr against NaBr. The number of ions in the ion atmosphere Cs^+ (red circles) versus Na^+ (gray circles); excluded Br^- anions are represented by the black triangles, and the total charge of the ion atmosphere summed from the individual ion measurements is shown as the black squares. (B) Competitive association of CsF against NaF. The number of ions in the ion atmosphere Cs^+ (red circles) versus Na^+ (gray circles); excluded F^- anions are represented by the open triangles and were estimated based on eq 1. Each data point is the average of 3−5 independent measurements. The lines at Γ = +46 represent the charge needed to neutralize the total DNA charge of −46. The solid line (red and gray) are fits to the Hill equation to provide an empirical guide. Error bars as in Figure 2. See Tables S13−S14 in Supporting Information for raw data.

bp DNA than Cs^+ ions (22.5 ± 1.4 Na^+ vs 11 ± 1.2 Cs^+, with ∼14 ± 1.4 Br^- anions excluded). The opposite effect was observed for 300 mM CsF and NaF salts; these gave an excess of 14 ± 1.6 Na^+ and 20 ± 1.3 Cs^+ ions (and 12 ± 1.8 F^- anions excluded, estimated based on eq 1). This result indicates that the anion identity can affect the cation occupancy of the ion atmosphere. As observed previously,[51] the anion effects mirror activity effects: CsBr has lower activity than NaBr and Cs^+ is less present in the ion atmosphere with Br^- as the anion, whereas the opposite holds for CsF and NaF (Figures S20 and S21; Table S25). In summary, the cations present in the ion atmosphere are strongly dependent on the anion identity, but only at high salt concentrations, as expected for an activity and ion association-based phenomenon.[73] At low and moderate concentrations (below 100 mM), monovalent cations occupy the ion atmosphere independent of size and anion identity (Figure S18 and Figure S22), as the nonideal effects become substantial only at higher concentrations.[51]

The prior studies that showed a preference for smaller cations were carried out at even higher salt concentrations,[53,54,56,57,63,71] concentrations too high to obtain accurate ion counting results. We therefore looked for a system to probe cation size and activity effects under the conditions of these experiments. For example, the tethered DNA relaxation study[53] was carried out with Cl^-, which could have preferentially associates with the larger cations[85] to give activity and ion pairing effects analogous to those described above and in ref 51 to account for the observed cation size preferences. However, these effects were small, the small-angle X-ray scattering readout for relaxation is complex and tethered DNA relaxation is not two-state, so we decided to look for a different experimental system to probe these effects.

The P4−P6 domain, derived from the *Tetrahymena* group I intron,[9,10,63,74,75] is 160 nucleotides long and forms a stable, closely packed structure stabilized by two tertiary contacts: the metal core-metal core receptor (MC-MCR) and the tetraloop-tertaloop receptor (TL-TLR) (Figure 9A). We used this system because its folding is two-state and because there is a well-established single molecule FRET (smFRET) assay[64,65,76] that gives high accuracy and precision.

In P4−P6, the MC-MCR preferentially binds divalent cations, and the TL-TLR is more stable in the presence of Na^+ or K^+ as the solution monovalent cation.[9,62,77−80] In the present study, we were primarily interested in understanding how monovalent ions within the RNA ion atmosphere alleviate unfavorable electrostatic repulsions during RNA folding; hence, we deliberately chose conditions that prevents the formation of MC/MCR[78] and used a mutant in the TL/TLR tertiary motif (A225U) that disrupts a monovalent cation-binding site[63] (see also refs 79, 81) (Figure 9B).

Figure 9C shows folding and unfolding rate constants and the equilibrium folding for A225U P4−P6 in a series of monovalent salts in the concentration range 1.8−2.9 M. Overall, the folding of A225U mutant of P4−P6 RNA is less favorable compared to wild-type P4−P6 RNA by nearly 2 orders of magnitude, as observed previously.[63] The A225U P4−P6 folding equilibrium constant was the same, within experimental error, in the presence of NaCl, KCl, or RbF (at 2.5 M, K_{eq}^{obs} = 0.45 ± 0.13, 0.38 ± 0.03, and 0.48 ± 0.03 for NaCl, KCl, and RbF, respectively). However, the folding equilibrium constant was ∼5-fold lower in the presence of RbCl (K_{eq}^{obs} = 0.09 ± 0.01 at 2.5 M). This differential effect appears to arise predominantly from a folding rather than unfolding effect (Figure 9C), consistent with less effective screening in RbCl, although there is more scatter in the individual rate constants than in the equilibrium measurements.

NaCl, KCl, and RbF solutions have similar activities, but the activity of RbCl solutions is lower (by 18% at 2.0 M, Table S25), due at least in part to the formation $Rb^+{\cdot}Cl^-$ ion pairs.[73,82,83] To take into account the differences in nonideal behavior of cations and anions, the folding rate and equilibrium constants for A225U P4−P6 were plotted as a function of salt activity, which expresses the effective concentration of free ions in the bulk solution (Figure 9D). The dependencies were essentially the same in all salts, suggesting that monovalent cations are equally adept at electrostatic screening and that the observed differences arise from activity and ion pairing effects.[51,73,82,83] The electrostatic relaxation of the tethered DNA duplexes[53] also correlates with the activity effects of the salts used in that study (Figure S23), further underscoring that the prior results do not provide evidence for cation size effects on electrostatic screening.

■ DISCUSSION

Models of the ion atmosphere have highlighted the presence of cations in the helical grooves of DNA and, in line with the restricted size of these grooves, differential occupancy of cations of different size.[31,32,36,37,39,41,44,84−90] It has also been suggested that stronger interactions of smaller cations with phosphoryl oxygen atoms favor smaller cations in the ion atmosphere.[30,31,37,40,41]

Our experimental results suggest, surprisingly, that ion atmosphere occupancy by monovalent cations is insensitive to the cation size across the alkali metal ions Na^+, K^+, Rb^+, and Cs^+. The simplest interpretation of our results is that the occupancy of these cations in the minor and major groove is low and that direct binding to phosphate backbone is weak, a model also consistent with the observation from quadrupolar cation NMR that ions within the ion atmosphere remain well hydrated.[91] Alternatively, solvated cations could have very similar phosphate interactions, as the stronger solvation of

DOI: 10.1021/jacs.6b04289
J. Am. Chem. Soc. 2016, 138, 10925−10934

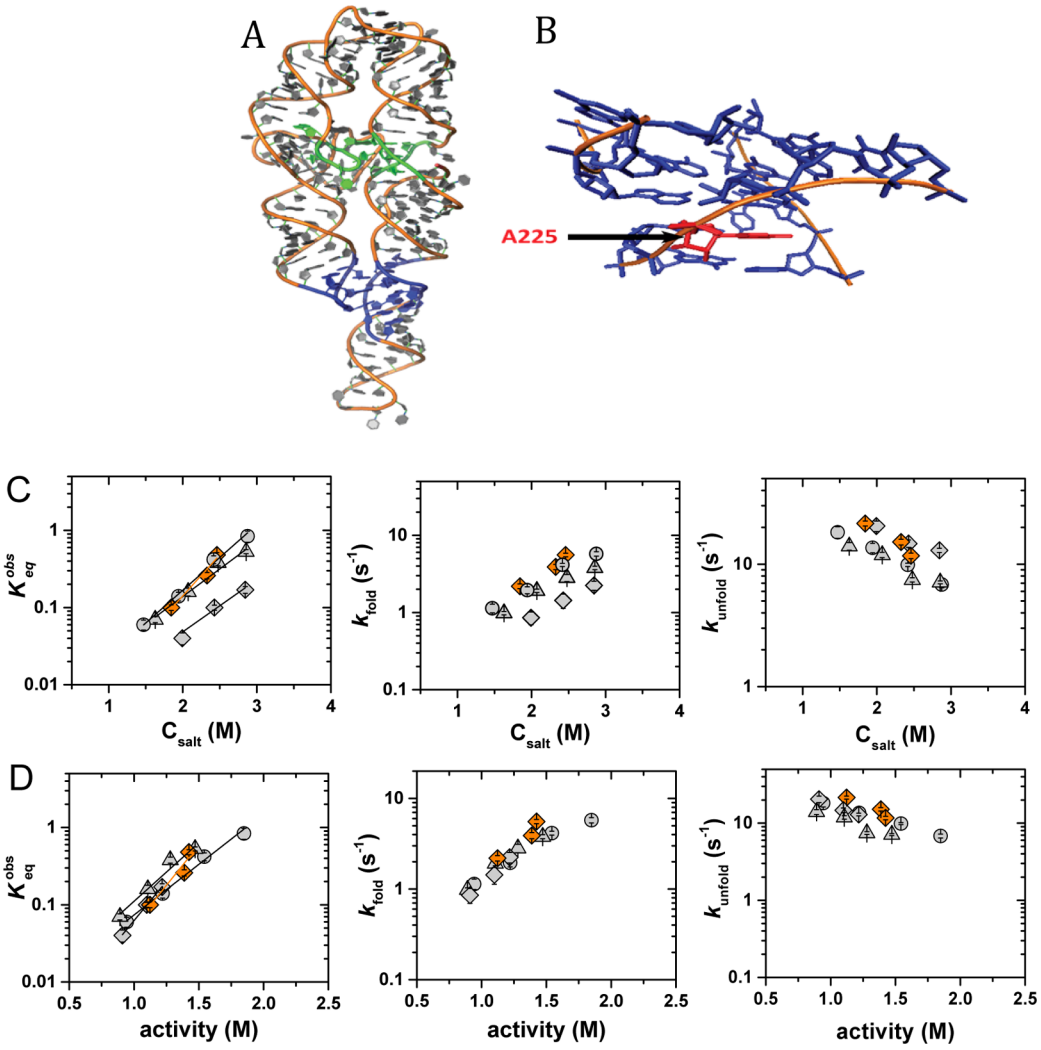

Figure 9. Folding kinetics and thermodynamics of the A225U mutant of P4−P6 RNA as a function of monovalent salt identity. (A) Structure of the P4−P6 domain of the Tetrahymena group I intron. Tertiary contacts are colored as follows: the tetraloop/tetraloop receptor (blue), and the metal core/metal core receptor (green); rendering based on the PDB: 1GID.[77] (B) Tetraloop/tetraloop receptor with a mutation site A225 indicated in red; rendering based on the PDB 1GID. (C) Equilibrium constant, folding and unfolding rate constants for folding of A225U P4−P6 RNA folding as a function of monovalent salt concentration. Salts containing Cl^- anion are presented in gray with different symbols correspond to a different cation: Na^+ (gray circles), K^+ (gray triangles), Rb^+ (gray diamonds). RbF is indicated by orange diamonds. (D) Plots and symbols as in (C) except plotted as a function of salt activity instead of concentration. The folding equilibrium is defined as the ratio of the folding rate constant to unfolding rate constant: $K_{eq}^{obs} = \frac{[Fold]}{[Unfold]} = \frac{k_{fold}}{k_{unfold}}$. The folding equilibrium constants were fitted to a straight line as an empirical guide. Error bars correspond to the bootstrap-estimated 95% confidence intervals (SD = 2σ). See Tables S21−S24 in Supporting Information for raw data and data summaries.

smaller cations could compensate for the higher charge density of the cation itself,[92] or there might be interactions with partially dehydrated cations, with the stronger interactions of smaller cations compensated by more facile dehydration of larger cations. Significantly different binding of TBA^+ (3-fold weaker compared to Na^+) might be attributed to its larger size, lower charge density, and/or the distinct hydration of its hydrophobic "shell".[93]

Draper and co-workers observed differential effects on RNA tertiary stability in the presence of different monovalent cations,[81] and monovalent cation interactions might be expected to be particularly common in the complex "nooks and crannies" of junctions and tertiary interactions. The absence of such effects on helix ion atmospheres, as observed herein, may aid in dissecting and understanding specific and general cation effects on RNA folding, association, and function.

Li^+ was the only alkali metal cation for which a preference was observed. The preference was ~25% over the other cations, highly reproducible, and observed across several different types of competition experiments (Figures 2, 4 and S16). Given the high charge density of Li^+, its preference may arise from direct interactions with a small subset of the anionic phosphoryl oxygen atoms, with such interactions being considerably weaker and below detection for the larger alkali metal ions.[83,94−96] The observed preference of ~2−4 Li^+ ions at equimolar Na^+ would, most simply, suggest interactions of Li^+ with ~5−10% of the phosphoryl groups (Figure 2A). Alternatively, some or all of the preferential Li^+ occupancy could occur in the helical grooves. Additional experimental approaches that allow direct assessment of such interactions will be needed to test these models and whether the preferentially associated Li^+ is partially dehydrated.

DOI: 10.1021/jacs.6b04289
J. Am. Chem. Soc. 2016, 138, 10925−10934

Given the extraordinary complexity and highly dynamic nature of the ion atmosphere, it is hard to imagine achieving the needed level of understanding in the absence of a strong theoretical foundation and accurate computational models. Traditionally, computational biology approaches have matched prior experimental observations. While this is likely a necessary step in model development, the agreement of a model with the data used to develop the model cannot be taken as support for the model's validity as highlighted by observations in the field of protein folding.[97,98] Early protein folding algorithms were developed by training on a portion of the known folded structures and validating against a subset of the data that were set aside for this purpose. However, such seemingly validated models, when confronted with the challenge of making blind predictions through the CASP cooperative, were unable to provide accurate structural predictions.[99−102]

Against this backdrop, the blind predictions for ion competition for DNA and RNA helixes made by York and colleagues[41] is extraordinarily valuable. These predictions have allowed us to experimentally evaluate the 3D-RISM ion atmosphere model in an unbiased manner. Our results indicate that the predicted 2-fold preferential occupancy of the ion atmosphere by Na^+ over Cs^+ around DNA and RNA helices does not hold (Figure 6). Thus, at a minimum, some aspect of the 3D-RISM models requires adjustment. The 3D-RISM model uses molecular mechanical force fields for solute−solvent and solvent−solvent interactions, but it has been recognized that the model predicts slightly stronger binding of cations to phosphoryl groups on the backbone compared to those from MD simulations.[32] This difference could arise if the SPC/E rigid water model does not accurately represent the hydration of cations within the ion atmosphere. Our results will help guide the development of these next-generation models, and analogous ion counting and additional experiments will allow evaluation of these models.

Other evidence for cation size effects came from electrostatic relaxation and similar experiments, but, as we have noted, these experiments were carried out, by necessity, at salt concentrations in the range 0.1−2.0 M[53−57] and recent experiments indicate that nonideal electrolyte behavior can alter ion atmosphere occupancy and presumably also affect screening.[51] To test electrostatic screening effects under these high salt conditions we turned to precise smFRET measurements of the folding of P4−P6 RNA. Our results demonstrate that the identity of the anion can affect folding and that salt activity differences can account for folding differences observed under these conditions (Figures 9C, 9D, and S22).

The above analyses and observations underscore the need for cycles that entail developing models, making testable predictions from those models, and testing those predictions through experimental observation. Indeed, these cycles are at the core of the scientific method,[103−106] and will help the field of nucleic acid electrostatics move forward. Correspondingly, there will be an increased need for experimental methods that can be unambiguously related to computational results, like ion counting, but provide more detailed information about the ion atmosphere shape and dynamics and its energetic consequences.

■ ASSOCIATED CONTENT

Supporting Information

The Supporting Information is available free of charge on the ACS Publications website at DOI: 10.1021/jacs.6b04289.

Figures S1−S23; Tables S1−S25 (PDF)

■ AUTHOR INFORMATION

Corresponding Author

*herschla@stanford.edu

Present Address

⊥Whitehead Institute for Biomedical Research, Cambridge, Massachusetts 02142, United States.

Notes

The authors declare no competing financial interest.

■ ACKNOWLEDGMENTS

We thank members of the Herschlag lab, Benjamin Allred, Mary Clay, Rhiju Das, Dawn Kellogg, and Ross Jay Metzger for helpful discussions and for critical advice. This work was supported by the National Institute of Health (grant P01GM066275 to D.H.).

■ REFERENCES

(1) Deng, H.; Bloomfield, V. A. *Biophys. J.* **1999**, *77*, 1556.
(2) Carrivain, P.; Cournac, A.; Lavelle, C.; Lesne, A.; Mozziconacci, J.; Paillusson, F.; Signon, L.; Victor, J. M.; Barbi, M. *Soft Matter* **2012**, *8*, 9285.
(3) Kornyshev, A. A.; Leikin, S. *Proc. Natl. Acad. Sci. U. S. A.* **1998**, *95*, 13579.
(4) Kornyshev, A. A.; Leikin, S. *Biophys. J.* **2013**, *104*, 2031.
(5) Yu, T. Y.; Schaefer, J. *J. Mol. Biol.* **2008**, *382*, 1031.
(6) Sun, S. Y.; Rao, V. B.; Rossmann, M. G. *Curr. Opin. Struct. Biol.* **2010**, *20*, 114.
(7) Draper, D. E. *Biophys. J.* **2008**, *95*, 5489.
(8) Leipply, D.; Draper, D. E. *Biochemistry* **2011**, *50*, 2790.
(9) Takamoto, K.; Das, R.; He, Q.; Doniach, S.; Brenowitz, M.; Herschlag, D.; Chance, M. R. *J. Mol. Biol.* **2004**, *343*, 1195.
(10) Silverman, S. K.; Cech, T. R. *RNA* **2001**, *7*, 161.
(11) Lipfert, J.; Doniach, S.; Das, R.; Herschlag, D. *Annu. Rev. Biochem.* **2014**, *83*, 813.
(12) Record, M. T., Jr.; Zhang, W.; Anderson, C. F. *Adv. Protein Chem.* **1998**, *51*, 281.
(13) Draper, D. E. *RNA* **2004**, *10*, 335.
(14) Wyman, J.; Gill, S. J. *Binding and Linkage: Functional Chemistry of Biological Macromolecules*; University Science Books: Mill Valley, CA, 1990.
(15) Manning, G. S. *J. Chem. Phys.* **1969**, *51*, 934.
(16) Manning, G. S. *Q. Rev. Biophys.* **1978**, *11*, 179.
(17) Sharp, K. A.; Honig, B. *J. Phys. Chem.* **1990**, *94*, 7684.
(18) Sharp, K. A. *Biopolymers* **1995**, *36*, 227.
(19) Misra, V. K.; Draper, D. E. *J. Mol. Biol.* **1999**, *294*, 1135.
(20) Lebret, M.; Zimm, B. H. *Biopolymers* **1984**, *23*, 287.
(21) Auffinger, P.; Westhof, E. *J. Mol. Biol.* **2000**, *300*, 1113.
(22) Rocchia, W.; Alexov, E.; Honig, B. *J. Phys. Chem. B* **2001**, *105*, 6507.
(23) Dolinsky, T. J.; Nielsen, J. E.; McCammon, J. A.; Baker, N. A. *Nucleic Acids Res.* **2004**, *32*, W665.
(24) Mills, P.; Anderson, C. F.; Record, M. T. *J. Phys. Chem.* **1985**, *89*, 3984.
(25) Tan, Z. J.; Chen, S. J. *J. Chem. Phys.* **2005**, *122*, 044903.
(26) Howard, J. J.; Lynch, G. C.; Pettitt, B. M. *J. Phys. Chem. B* **2011**, *115*, 547.
(27) Feig, M.; Pettitt, B. M. *Biophys. J.* **1999**, *77*, 1769.
(28) Cheatham, T. E.; Young, M. A. *Biopolymers* **2000**, *56*, 232.
(29) Rueda, M.; Cubero, E.; Laughton, C. A.; Orozco, M. *Biophys. J.* **2004**, *87*, 800.
(30) Savelyev, A.; Papoian, G. A. *J. Am. Chem. Soc.* **2006**, *128*, 14506.
(31) Yoo, J.; Aksimentiev, A. *J. Phys. Chem. B* **2012**, *116*, 12946.
(32) Giambasu, G. M.; Luchko, T.; Herschlag, D.; York, D. M.; Case, D. A. *Biophys. J.* **2014**, *106*, 883.

DOI: 10.1021/jacs.6b04289
J. Am. Chem. Soc. 2016, 138, 10925−10934

(33) Pan, F.; Roland, C.; Sagui, C. *Nucleic Acids Res.* **2014**, *42*, 13981.
(34) Ponomarev, S. Y.; Thayer, K. M.; Beveridge, D. L. *Proc. Natl. Acad. Sci. U. S. A.* **2004**, *101*, 14771.
(35) Varnai, P.; Zakrzewska, K. *Nucleic Acids Res.* **2004**, *32*, 4269.
(36) Cheng, Y.; Korolev, N.; Nordenskiold, L. *Nucleic Acids Res.* **2006**, *34*, 686.
(37) Savelyev, A.; MacKerell, A. D. *J. Phys. Chem. B* **2015**, *119*, 4428.
(38) Savelyev, A.; MacKerell, A. D. *J. Phys. Chem. Lett.* **2015**, *6*, 212.
(39) Savelyev, A.; MacKerell, A. D. *J. Chem. Theory Comput.* **2015**, *11*, 4473.
(40) Savelyev, A.; Papoian, G. A. *J. Phys. Chem. B* **2008**, *112*, 9135.
(41) Giambasu, G. M.; Gebala, M. K.; Panteva, M. T.; Luchko, T.; Case, D. A.; York, D. M. *Nucleic Acids Res.* **2015**, *43*, 8405.
(42) Rouzina, I.; Bloomfield, V. A. *J. Phys. Chem.* **1996**, *100*, 4292.
(43) Savelyev, A.; Mackerell, A. *Biophys. J.* **2015**, *108*, 231A.
(44) Pasi, M.; Maddocks, J. H.; Lavery, R. *Nucleic Acids Res.* **2015**, *43*, 2412.
(45) Perez, A.; Marchan, I.; Svozil, D.; Sponer, J.; Cheatham, T. E., 3rd; Laughton, C. A.; Orozco, M. *Biophys. J.* **2007**, *92*, 3817.
(46) Joung, I. S.; Cheatham, T. E. *J. Phys. Chem. B* **2008**, *112*, 9020.
(47) Berendsen, H. J. C.; Grigera, J. R.; Straatsma, T. P. *J. Phys. Chem.* **1987**, *91*, 6269.
(48) Bai, Y.; Greenfeld, M.; Travers, K. J.; Chu, V. B.; Lipfert, J.; Doniach, S.; Herschlag, D. *J. Am. Chem. Soc.* **2007**, *129*, 14981.
(49) Das, R.; Mills, T. T.; Kwok, L. W.; Maskel, G. S.; Millett, I. S.; Doniach, S.; Finkelstein, K. D.; Herschlag, D.; Pollack, L. *Phys. Rev. Lett.* **2003**, DOI: 10.1103/PhysRevLett.90.188103.
(50) Kirmizialtin, S.; Pabit, S. A.; Meisburger, S. P.; Pollack, L.; Elber, R. *Biophys. J.* **2012**, *102*, 819.
(51) Gebala, M.; Giambasu, G. M.; Lipfert, J.; Bisaria, N.; Bonilla, S.; Li, G. C.; York, D. M.; Herschlag, D. *J. Am. Chem. Soc.* **2015**, *137*, 14705.
(52) Pabit, S. A.; Meisburger, S. P.; Li, L.; Blose, J. M.; Jones, C. D.; Pollack, L. *J. Am. Chem. Soc.* **2010**, *132*, 16334.
(53) Bai, Y.; Chu, V. B.; Lipfert, J.; Pande, V. S.; Herschlag, D.; Doniach, S. *J. Am. Chem. Soc.* **2008**, *130*, 12334.
(54) Bleam, M. L.; Anderson, C. F.; Record, M. T. *Proc. Natl. Acad. Sci. U. S. A.* **1980**, *77*, 3085.
(55) Stellwagen, E.; Dong, Q.; Stellwagen, N. C. *Biopolymers* **2005**, *78*, 62.
(56) Stellwagen, E.; Stellwagen, N. C. *Biophys. J.* **2003**, *84*, 1855.
(57) Zinchenko, A. A.; Yoshikawa, K. *Biophys. J.* **2005**, *88*, 4118.
(58) Greenfeld, M.; Herschlag, D. *Methods Enzymol.* **2009**, *469*, 375.
(59) Instrument stability was excellent such that no samples were removed or adjusted due to instrument drift.
(60) Bu, X. D.; Wang, T. B.; Hall, G. *J. Anal. At. Spectrom.* **2003**, *18*, 1443.
(61) Anderson, C. F.; Record, M. T. *J. Phys. Chem.* **1993**, *97*, 7116.
(62) Leipply, D.; Lambert, D.; Draper, D. E. *Methods Enzymol.* **2009**, *469*, 433.
(63) Bisaria, N.; Herschlag, D. *Biochem. Soc. Trans.* **2015**, *43*, 172.
(64) Sattint, B. D.; Zhao, W.; Travers, K.; Chut, S.; Herschlag, D. *J. Am. Chem. Soc.* **2008**, *130*, 6085.
(65) Greenfeld, M.; Pavlichin, D. S.; Mabuchi, H.; Herschlag, D. *PLoS One* **2012**, *7*, e30024.
(66) Mahler, J.; Persson, I. *Inorg. Chem.* **2012**, *51*, 425.
(67) Aue, D. H.; Webb, H. M.; Bowers, M. T. *J. Am. Chem. Soc.* **1976**, *98*, 12.
(68) The radii of the hydrated organic ions were approximated from the crystal radius (ref 67) plus 1.4 Å for a water layer.
(69) Titration of TMB^+ to Na^+ solution was not carried to the concentration where Na^+ was completely competed from the ion atmosphere. The value of α is therefore less precisely determined.
(70) The stock solution concentration of TMABr was assessed by quantifying the amount of Br^- in samples by ICP MS.
(71) Koculi, E.; Hyeon, C.; Thirumalai, D.; Woodson, S. A. *J. Am. Chem. Soc.* **2007**, *129*, 2676.
(72) Chen, A. A.; Draper, D. E.; Pappu, R. V. *J. Mol. Biol.* **2009**, *390*, 805.
(73) Robinson, R. A.; Stokes, R. H. *Electrolyte Solutions*, 2nd. rev. ed.; Dover Publications: Mineola, NY, 2002.
(74) Murphy, F. L.; Cech, T. R. *Biochemistry* **1993**, *32*, 5291.
(75) Deras, M. L.; Brenowitz, M.; Ralston, C. Y.; Chance, M. R.; Woodson, S. A. *Biochemistry* **2000**, *39*, 10975.
(76) Greenfeld, M.; Solomatin, S. V.; Herschlag, D. *J. Biol. Chem.* **2011**, *286*, 19872.
(77) Cate, J. H.; Gooding, A. R.; Podell, E.; Zhou, K. H.; Golden, B. L.; Kundrot, C. E.; Cech, T. R.; Doudna, J. A. *Science* **1996**, *273*, 1678.
(78) Das, R.; Travers, K. J.; Bai, Y.; Herschlag, D. *J. Am. Chem. Soc.* **2005**, *127*, 8272.
(79) Basu, S.; Rambo, R. P.; Strauss-Soukup, J.; Cate, J. H.; Ferre-D'Amare, A. R.; Strobel, S. A.; Doudna, J. A. *Nat. Struct. Biol.* **1998**, *5*, 986.
(80) Uchida, T.; He, Q.; Ralston, C. Y.; Brenowitz, M.; Chance, M. R. *Biochemistry* **2002**, *41*, 5799.
(81) Lambert, D.; Leipply, D.; Shiman, R.; Draper, D. E. *J. Mol. Biol.* **2009**, *390*, 791.
(82) Chen, A. A.; Pappu, R. V. *J. Phys. Chem. B* **2007**, *111*, 6469.
(83) Fennell, C. J.; Bizjak, A.; Vlachy, V.; Dill, K. A.; Sarupria, S.; Rajamani, S.; Garde, S. *J. Phys. Chem. B* **2009**, *113*, 14837.
(84) Hamelberg, D.; McFail-Isom, L.; Williams, L. D.; Wilson, W. D. *J. Am. Chem. Soc.* **2000**, *122*, 10513.
(85) Lavery, R.; Maddocks, J. H.; Pasi, M.; Zakrzewska, K. *Nucleic Acids Res.* **2014**, *42*, 8138.
(86) Hud, N. V.; Engelhart, A. E. In *Nucleic Acid-Metal Ion Interactions*; Hud, N. V., Ed.; Royal Society of Chemistry, 2008; p 75.
(87) Shen, X.; Atamas, N. A.; Zhang, F. S. *Phys. Rev. E* **2012**, DOI: 10.1103/PhysRevE.85.051913.
(88) Verma, S. D.; Pal, N.; Singh, M. K.; Sen, S. *J. Phys. Chem. Lett.* **2012**, *3*, 2621.
(89) Marincola, F. C.; Denisov, V. P.; Halle, B. *Abstr. Pap. Am. Chem. S.* **2003**, *225*, U466.
(90) Marincola, F. C.; Denisov, V. P.; Halle, B. *J. Am. Chem. Soc.* **2004**, *126*, 6739.
(91) Braunlin, W. H. *Adv. Biophys. Chem.* **1995**, *5*, 52.
(92) Marcus, Y. *J. Phys. Chem. B* **2005**, *109*, 18541.
(93) Stangret, J.; Gampe, T. *J. Phys. Chem. B* **1999**, *103*, 3778.
(94) Collins, K. D. *Biophys. J.* **1997**, *72*, 65.
(95) Collins, K. D.; Neilson, G. W.; Enderby, J. E. *Biophys. Chem.* **2007**, *128*, 95.
(96) Ganguly, P.; Schravendijk, P.; Hess, B.; van der Vegt, N. F. *J. Phys. Chem. B* **2011**, *115*, 3734.
(97) Moult, J.; Fidelis, K.; Kryshtafovych, A.; Rost, B.; Hubbard, T.; Tramontano, A. *Proteins: Struct., Funct., Genet.* **2007**, *69*, 3.
(98) Moult, J.; Fidelis, K.; Kryshtafovych, A.; Schwede, T.; Tramontano, A. *Proteins: Struct., Funct., Genet.* **2014**, *82*, 1.
(99) Bonneau, R.; Baker, D. *Annu. Rev. Biophys. Biomol. Struct.* **2001**, *30*, 173.
(100) Khoury, G. A.; Liwo, A.; Khatib, F.; Zhou, H. Y.; Chopra, G.; Bacardit, J.; Bortot, L. O.; Faccioli, R. A.; Deng, X.; He, Y.; Krupa, P.; Li, J. L.; Mozolewska, M. A.; Sieradzan, A. K.; Smadbeck, J.; Wirecki, T.; Cooper, S.; xxFlatten, J.; Xu, F.; Baker, D.; Cheng, J. L.; Delbem, A. C. B.; Floudas, C. A.; Keasar, C.; Levitt, M.; Popovic, Z.; Scheraga, H. A.; Skolnick, J.; Crivelli, S. N.; Players, F. *Proteins: Struct., Funct., Genet.* **2014**, *82*, 1850.
(101) Moult, J. *Curr. Opin. Struct. Biol.* **2005**, *15*, 285.
(102) Bourne, P. E. *Methods Biochem. Anal.* **2003**, *44*, 501.
(103) Barrow, J. D. *Scientist* **1990**, *4*, 13.
(104) Hempel, C. G. *Philosophy of Natural Science*; Prentice-Hall: Englewood Cliffs, NJ, 1966.
(105) Popper, K. R. *The Logic of Scientific Discovery*; Routledge: London, 1992.
(106) Popper, K. R.; Bartley, W. W. *Realism and the Aim of Science*; Routledge: London, 1993.

DOI: 10.1021/jacs.6b04289
J. Am. Chem. Soc. 2016, 138, 10925−10934